GEOLOGICA CARPATHICA, JUNE 2020, 71, 3, 274–287 https://doi.org/10.31577/GeolCarp.71.3.6

Zircon U–Pb geochronology from Permian rocks of the Tribeč Mts. (Western Carpathians, Slovakia)

ANNA VOZÁROVÁ[1, ✉], KATARÍNA ŠARINOVÁ[1], NICKOLAY RODIONOV[2] and JOZEF VOZÁR[3]

[1]Comenius University in Bratislava, Faculty of Natural Sciences, Department of Mineralogy and Petrology, Mlynská dolina, Ilkovičova 6, 842 15 Bratislava, Slovakia; ✉anna.vozarova@uniba.sk, katarina.sarinova@uniba.sk
[2]Centre of Isotopic Research, A.P. Karpinsky Russian Geological Research Institute (FGBU "VSEGEI"), Sredny prospekt 74, 199 106 St.-Petersburg, Russia; Nickolay_Rodionov@vsegei.ru
[3]Earth Science Institute of the Slovak Academy of Sciences, Dúbravská cesta 9, 840 05 Bratislava, Slovakia; jozef.vozar@savba.sk

(Manuscript received March 12, 2020; accepted in revised form May 6, 2020; Associate Editor: Igor Broska)

Abstract: U–Pb dating of magmatic zircons from the Permian basaltic metaandesites/metabasalts of the Tribeč Mts. yielded the Concordia ages of 263.1±2.6 Ma, which correspond to the Guadalupian Epoch in the time span of the uppermost Wordian/Capitanian Stages. These magmatic zircon ages clearly document the timing of the Mid-Permian lithospheric extension in the internal zone of the Variscan fragments in the Western Carpathians. The studied volcanic rocks with the associated metasediments belong to the Veporic Unit that overthrusts the Tatric Unit. The considered sequence was correlated with the Northern Veporic Permian rocks from the Čierťaž Mts. From the geochemical point of view, the studied volcanic rocks have a calc-alkaline magmatic trend with an affinity to continental within-plate tectonic setting, linked to the post-orogenic lithospheric extension. The detrital zircon population, obtained from the associated arkosic metagreywackes, displays mainly Tournaisian and Ediacaran zircon ages in the range of 342–367 and 546–631 Ma, respectively. Only a small number of Cambrian/Ordovician (499–466 Ma), Tonian (720–1000 Ma) and Paleoproterozoic/Neoarchean (~1.9 Ga and ~2.5 Ga) zircon ages were determined. The similar association of zircon ages was found within the xenocrystic cores in the studied volcanic rocks. The presented detrital and xenocrystic zircon ages specify the provenance of the Tribeč Permian deposits from the Western Carpathian Crystalline Basement crust, characteristic of derivation from the Variscan magmatic rocks and reworked fragments of Cadomian crust.

Keywords: SHRIMP zircon dating, Permian volcanism, geochemistry, provenance, Central Western Carpathians.

Introduction

Volcanic rocks and their volcaniclastics are common parts of the Late Paleozoic sedimentary sequences in the Western Carpathians (e.g., Vozárová & Vozár 1988 and references therein; Biely et al. 1996). To a large extent, the majority of the Pennsylvanian and Permian sediments arose in continental sedimentary environments and consequently, the biostratigraphic evidence for their age is lacking or only very uncertain. For this reason, the age dating of the associated volcanic or pyroclastic rocks has proved to be important in terms of determining the age of these sedimentary sequences. These age data are significant in terms of their correlation with other occurrences in the Western Carpathians. Recently, the isotopic age data of the Permian or Permian–Triassic volcanites have also increased from occurrences in the Western Carpathians, mainly based on the age dating of zircons and monazites (e.g., – Kotov et al. 1996; Rojkovič & Konečný 2005; Vozárová et al. 2008, 2009, 2012, 2015, 2016; Demko & Hraško 2013; Putiš et al. 2016; Pelech et al. 2017; Ondrejka et al. 2018). Kohút et al. (2013) documented Re–Os molybdenite ages on the U–Mo deposit from the Permian volcanites of the Northern Gemeric Unit.

It is obvious that any new age data from Permian volcanites is welcome and will help to illustrate the overall picture of the development and paleogeography of the Late Paleozoic sequences in the Western Carpathians. For this reason, our attention was focused on a small volcanic body in the midst of Permian sediments in the Tribeč Mts., in order to determine the age of the volcanism and its correlation with other occurrences in the Western Carpathians.

Three samples have been processed for zircon dating from the Permian rocks of the Tribeč Mts. succession (Fig. 1; Table 1), two of them from the volcanic horizon (samples *T-1* and *T-2*) and another from the associated sediments, to find out the assemblage of detrital zircons (sample *T-3*). For better knowledge of these volcanic rocks, chemical analyses were also performed, from sample *T-1* (andesite pyroclastic rock) and from samples *T-13A, B* (basaltic andesites/basalts).

Geological background

The Western Carpathian orogenic belt consists of several northward-stacked crustal-scale superunits and several cover nappe systems (Andrusov 1968; Maheľ 1986; Biely et al. 1996; Plašienka et al. 1997; Rakús et al. 1998; Plašienka 2018 and references therein). Based on the latest geological synthesis, a triple regional division of the Western Carpathians is used: the Internal, Central and External Western Carpathians

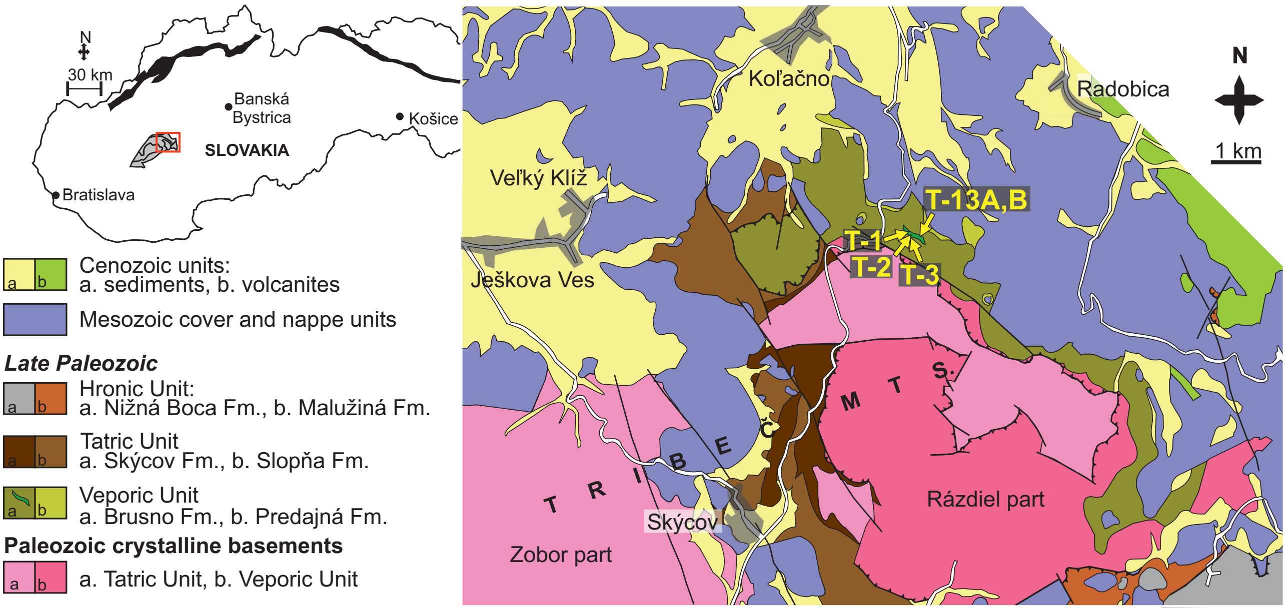

Fig. 1. Geological map of the Tribeč Mts. showing the localities of magmatic and detrital zircon samples, modified according to the Geological map of Tribeč, 1:50.000, after Ivanička et al. 1998; studied area location in the simplified map of Slovakia.

Table 1: List of analysed Permian rocks from the Tribeč Mts. with location of samples and GPS coordinates.

Sample	Sample locality	GPS coordinates
T-1	right slope of Šaloviny, ca 750 W from Kostelný vrch elevation (632 m), cliff overhead forest road, 370 m above sea level	48°33.497'N, 18°27.463'E
T-2	S of the Veľké Uherce village, Drahožická dolina Valley, abandoned quarry, 379 m above sea level	48°33.484'N, 18°27.523'E
T-3	S of the Veľké Uherce village, Drahožická dolina Valley, abandoned quarry, 374 m above sea level	48°33.484'N, 18°27.520'E
T-13A, B	Right slope of Šaloviny, forest road cut, 430 m above sea level	48°33.490'N, 18°27.460'E

(Rakús et al. 1998; Plašienka 2018 and references therein). The Tribeč Mts. rock complexes are placed in the Central Western Carpathians (CWC) zone and represent the westernmost promontory of the so-called Core Mountains. Cropping out from the Tertiary sediments of the Danube Basin the Tribeč Mts. form a NE–SW striking horst divided by the Skýcov fault system (Fusán et al. 1987) into the northern Rázdiel Part and the southern Zobor Part. The composite geological structure of the Tribeč Mts. comprises the crystalline basement rocks of the Tatric Unit and their Permian–Mesozoic envelope sequence, the Veporic crystalline basement with its Permian–Mesozoic envelope assemblage, the Carboniferous–Permian and Triassic rock complexes of the Hronic Unit, as well as a scarce Triassic nappe outlier of the highest superficial Strážov Nappe (Biely 1974, 1977; Ivanička et al. 1998 and references therein).

The studied area for the zircon age dating is situated in the Rázdiel Part of the Tribeč Mts., in the Veporic Unit (Fig. 1). The oldest stratigraphic horizon of the Veporic Unit is represented by crystalline rocks, mainly consisting of mica schists, phyllites, amphibolites and granitoids. Two tectonic slices were distinguished within this crystalline basement, the lower, mainly comprising mica schists with lenses of amphibolites, and the upper, including different types of granitoid rocks (Ivanička et al. 1998 and references therein). Generally, the whole crystalline basement rocks show retrograde features due to strong Alpine reworking.

Permian sediments overlapped unconformably the complex of granitoids and their blastomylonites, indicating a long brake in sedimentation after the Variscan tectono–thermal cycle. They are mostly represented by the light green arkosic metagreywackes, with intercalations of conglomerate layers in some places. Generally, the Permian sedimentary complex consists of multiple repetition of tabular bodies of sandstones and fine-grained sandy conglomerates of variable thickness. Erosive contacts are frequent. Sedimentary structures indicate an environment of low-sinuosity rivers characterized by networks of braided distributary channels transporting abundant coarse-sandy material. Frequent washouts, erosive channels, as well as poorly preserved fine-grained sediments are taken as evidence of quick and chaotic changes of braided channels with autocyclic erosive processes. The following rocks were recognized within the pebble material: microgranites, porphyric granitoids, vein quartz and light orthogneisses. Dominant mineral component of the arkosic metasandstones (n=4) is quartz (54 %), followed by K-feldspars (18 %), plagioclases

(11 %), lithic rock fragments (12 %) and detrital micas (5 %) (Vozárová in Ivanička et al. 1998). Among sandy grade lithic fragments, the following were distinguished; dacites, andesites, aplitic granitoids and mica schists. Thin lenses of volcaniclastic, together with several andesite/basalt lava flows were identified within the arkosic metasediments. Similar types of volcanites in the Tribeč Mts. were first time mentioned by Ďurovič et al. (1992). This horizon of arkosic metasediments with occurrences of intermediate volcanites was correlated by Vozár & Vozárová (1988; in Ivanička et al. 1998) with the Permian sediments of the Northern Veporic Unit that were originally defined as the Brusno Formation (Vozárová 1979).

The sequence of dark-violet metagreywackes and sandy shales represents the youngest Permian sediments in the Tribeč Mts. They appear in the form of erosive residues overlying the Brusno Formation arkosic metagreywackes and direct underlie the highly quartzose Lower Triassic sediments. They were correlated with the Predajná Formation from the Northern Veporic Unit (in the sense of Vozárová 1979). Their superposition and significant differences in the mineral composition with respect to the Lower Triassic sediments make it possible to assume a substantial brake in sedimentation between the Permian and the Lower Triassic period.

The Mesozoic part of the Veporic envelope in the Tribeč Mts. is represented by a complete lithostratigraphic sequence, beginning with the Lower Triassic quartzites and ending with the Albian flysch-like Poruba Beds (Polák in Ivanička et al. 1998). The entire sequence is affected by the Alpine deformation and recrystallization.

The Mesozoic envelope sequence of the Veporic Unit in the Tribeč Mts. shows a strong affinity to the envelope of the Northern Veporic Unit in the eastern part of the Nízke Tatry Mts. (Veľký Bok Sequence; Biely et al. 1997). Polák (in Ivanička et al. 1998) designated this Veporic Mesozoic envelope in the Tribeč Mts. as the Veľké Pole Sequence.

Analytical methods

The rock-forming minerals were studied by the electron microprobe JEOL JXA 8530OF, in the Laboratory of Electron Microanalysis (EMPA) of the Earth Science Institute of the Slovak Academy of Sciences, division Banská Bystrica. The zircons were extracted from the rocks by standard grinding, heavy liquid and magnetic separation techniques. The internal structure of individual zircon crystals was examined with cathodoluminescence (CL) imaging by SEM (CamScanM2500 Oxford Instruments). In situ U–Pb analyses were performed using a Sensitive High-Resolution Ion Microprobe (SHRIMP-II) at the Centre of Isotopic Research (CIR) in the A.P. Karpinsky Russian Geological Institute (VSEGEI), by applying a secondary electron multiplier in peak-jumping mode, based on the procedure described by Williams (1998). Primary beam diameter allowed the analysis an area of c. 25×20 μm. Cathodoluminescence (CL), backscattered electrons (BSE) and optical (transmitted light) imaging was applied to reveal the internal and surface features that were used to choose the position of analytical spots on the mostly homogeneous inclusion-free parts of individual zircon grains. The 80 μm wide ion source slit, in combination with a 100 μm multiplier slit, allowed for the mass-resolution $M/\Delta M \geq 5{,}000$ (1 % valley); hence, all the possible isobaric interferences were resolved. The following ion species were measured in the sequence: $^{196}(Zr_2O)$–^{204}Pb–background (c. 204.5 AMU)–^{206}Pb–^{207}Pb–^{208}Pb–^{238}U–^{248}ThO–^{254}UO. At least 4 mass-spectrums were acquired for each analysis. Zircon Temora-1 (Black et al. 2003) was measured as the main reference material (RM): one analysis per every four analyses of unknowns to obtain their U/Pb ratios. Zircon 91500 (Wiedenbeck et al. 1995) was used as a concentration RM. The obtained results were processed by the SQUID v1.12 (Ludwig 2005) and ISOPLOT/Ex 3.75 (Ludwig 2012) software, with decay constants recommended by Steiger & Jäger (1977), including modern corrections such as Hiess et al. (2012). Common lead correction was done on the basis of the measured $^{204}Pb/^{206}Pb$ ratio. The ages given in this text, if not additionally specified, are $^{207}Pb/^{206}Pb$ for zircon older than 1.0 Ga, and $^{206}Pb/^{238}U$ for those younger than 1.0 Ga. The degree of discordance was calculated according to the following formula: $\% D=100*(Age^{207/206}/Age^{206/238}-1)$. The uncertainties are quoted at standard deviation level (1σ, i.e. 68.3 % confidence) for individual points and at 2σ level in the Concordia diagram, for the Concordia ages or any previously published ages discussed in the text. Age distributions of detrital zircons are displayed as Kernel Density Estimates (Vermeesch 2018). Only analyses that overlay Concordia line within individual uncertainties were used for concordant-age calculation. The time-scale calibration of the International Chronostratigraphic Chart (2019-05) was used to compare geochronological data from detrital zircons with fossil-bearing sedimentary units and tectono-thermal events.

The chemical composition of the *T-1* rock was analysed at the ACME Analytical Laboratories (Vancouver, Canada). The chemical compositions of the *T-13A, B* samples were analysed at the Geoanalytical Laboratories of State Geological Institute of Dionýz Štúr (Bratislava – Spišská Nová Ves, Slovakia). Major elements were determined by inductively coupled plasma emission spectrometry (ICP) and trace and rare earth elements by inductively coupled plasma mass spectrometry (ICP-MS).

Sample characteristics

Volcanic rocks

Petrography: Sample *T-1* represents the pyroclastic rock which forms a layer inside the arkosic metasediments within the surface outcrop. Compositionally and texturally, it corresponds to the andesitic lapilli metatuff with lithic, vitric and crystal fragments. Lithic fragments are represented by the andesite with porphyric or intersertal microtexture. Among the studied crystals were plagioclases with a composite twinning (Albite and Pericline laws), strong altered biotite and scarce amphibole, and relatively less β-quartz. It should be noted that practically all plagioclases are altered only to albite. The studied rock is dark violet unevenly foliated, with foliation obliterated in the initial matrix texture, the former rich in vitric splinters. Due to the strong Alpine deformation, the interstices between volcanic lithic and crystal fragments are occupied by foliated crystalline aggregates of chlorite and Fe–Ti oxides, associated with sericite, albite and quartz.

Basaltic metaandesites/metabasalts are represented by the samples *T-2* and *T-13A, B*. They are fine-grained, solid dark-violet rocks,, slightly deformed and foliated, to some extent of crenulation cleavage. Characteristic is porphyritic texture with intersertal and fluidal groundmass. The mineral composition includes phenocryst of plagioclases, highly hematitized mafic minerals, and vastly resorbed β-quartz.

The plagioclases show repeated twins on the Albite and/or the Pericline laws. Albite-Carlsbad twinning is relatively common. The euhedral to anhedral plagioclases are broken and very often deformed along foliation planes, intensively altered to albite and replaced by secondary muscovite and calcite. The alteration rate varies depending on the anorthite content, with the larger anorthite contents being more completely altered than the zones rich in the albite component. Sieve texture were observed in the edges of plagioclase phenocrysts. This would be caused by heating events such as magma mixing, during which the temperature of magma was temporarily higher than the solidus of some minerals (Tsuchiyama & Takahashi 1983; Stewart & Pearce 2004). Nelson & Montana (1992) described the origin of sieve-plagioclases in connection with the rapid decompression, which may ultimately also be related to magma mixing.

Mafic phenocrysts are totally replaced by chlorite, sericite and Fe–Ti oxide/hydroxide, epidote/zoisite and dolomite.

Beta-quartz phenocrysts show distinct magmatic corrosion. Individual quartz crystals have embayed margins and are wrapped by fine aggregates of chlorite and opaque minerals. Quartz crystals are mostly anhedral, assumed due to magmatic resorption. They are also extensively fractured with slight oscillatory zoning in some places, often truncated by resorption surfaces. Resorbed and embayed quartz crystals with dissolution surfaces are found throughout the whole texture.

Recrystallized matrix consists of fine-grained, considerably preferred aggregate of chlorite, Fe-oxide/hydroxide minerals, calcite, albite, quartz, sericite and rarely epidote. Fine needles of rutile and crystals of apatite are frequent. Laths and needles of plagioclases are replaced by albite and sericite. Magnetite and ilmenite were detected as primary magmatic phases, either as inclusions in the mafic phenocrysts or as individual grains in the groundmass.

Geochemistry: Immobile trace elements such as high field strength elements (HFSE) and rare elements (REEs) have been used to classify of rocks and monitor magmatic affinities. These elements are less sensitive to alteration and hydrothermal overprint. Representative major- and trace elements including REEs are given in Supplementary Table S1. A list of the analysed volcanic rocks and sample localities is given in Table 1. Data plotted on the diagram after Winchester and Floyd (1977) modified by Pearce (1996), using the ratio of immobile trace elements Zr/Ti vs Nb/Y, show a sub-alkaline affinity for all samples (Fig. 2a). Within the plot, the samples *T-13A, B* clustered near the boundary between basaltic andesite/basalt fields with clear basalt affinity. The sample *T-1* falls within basaltic andesite/andesite field with higher Zr/Ti ratios compared to the rocks from group 1. Following the techniques proposed by MacLean & Barrett (1993), the immobile element ratios Zr/Y indicate a distinct calc-alkaline magmatic trend for all studied samples, ranging from 6.3 to 7.7. Equally, the Th/Yb ratios (1.43–1.48 for basalts and 4.94 for pyroclastic rock) clearly specify the calc-alkaline magmatic trend.

The chondrite normalized (Sun & McDonough 1989) REE patterns (Fig. 2b) shows enrichment in light REEs (LREEs) and has a slightly negative to flat pattern on the heavy REEs (HREEs). The enrichment in LREEs is indicated by relatively higher La_N/Yb_N ratios, 12.2 for the sample *T-1* and 7.7–7.9 for the samples *T-13A* and *T-13B*, respectively. Only indistinct negative Eu anomalies were observed, with 0.75 for sample *T-1* and 0.77–0.79 for samples *T-13A* and *T-13B*.

To deduce further the origin and source of these rocks, tectonic discrimination diagram (after Pearce 1983 revised by Gorton & Schandl 2000) was used, plotting ratios of Th/Yb vs Ta/Yb and Ta/Th vs Yb (Fig. 2c, d). These data strongly suggest a Within Plate Volcanic Zone (WPVZ) tectonic setting.

Sedimentary rocks

Petrography: Arkosic metagreywackes, surrounding the volcanogenic horizon, are represented by the sample *T-3*. This sample comes from the direct underlier of the volcanogenic horizon. Its light-grey or light green-grey colour and highly foliated structure are characteristic. They are poorly sorted, containing coarse grains of quartz, feldspars, detrital micas and dark-violet volcanic fragments stretched along the foliation planes. Quartz is dominant in rock composition (~50 %), mostly in coarse-grained polycrystalline varieties. The second important component is feldspars (~35 %), including K-feldspars (~18 %) and plagioclases (~17 %). Generally, they are secondary altered in variable intensity, and are replaced by aggregate of sericite, albite and rarely calcite. The plagioclase relics composition ranges up to $An_{15.5}$ (Supplementary Table S2). Due to the strong albitization, Ca-richer phases are preserved either in central parts of the previous plagioclase crystals or in the form of unevenly spotted patches throughout the whole crystal. The alteration processes, most likely pre-sedimentary magmatic/post-magmatic and/or diagenetic, transform the composition of Ca-rich plagioclases to Na-rich albite phases. Besides essentially Na and Ca variations the plagioclases contain insignificant orthoclase component content, varying up to 1.8 molar percent. Other elements which are present in very limited amounts include Fe, Mg, Mn, Ba, and Sr.

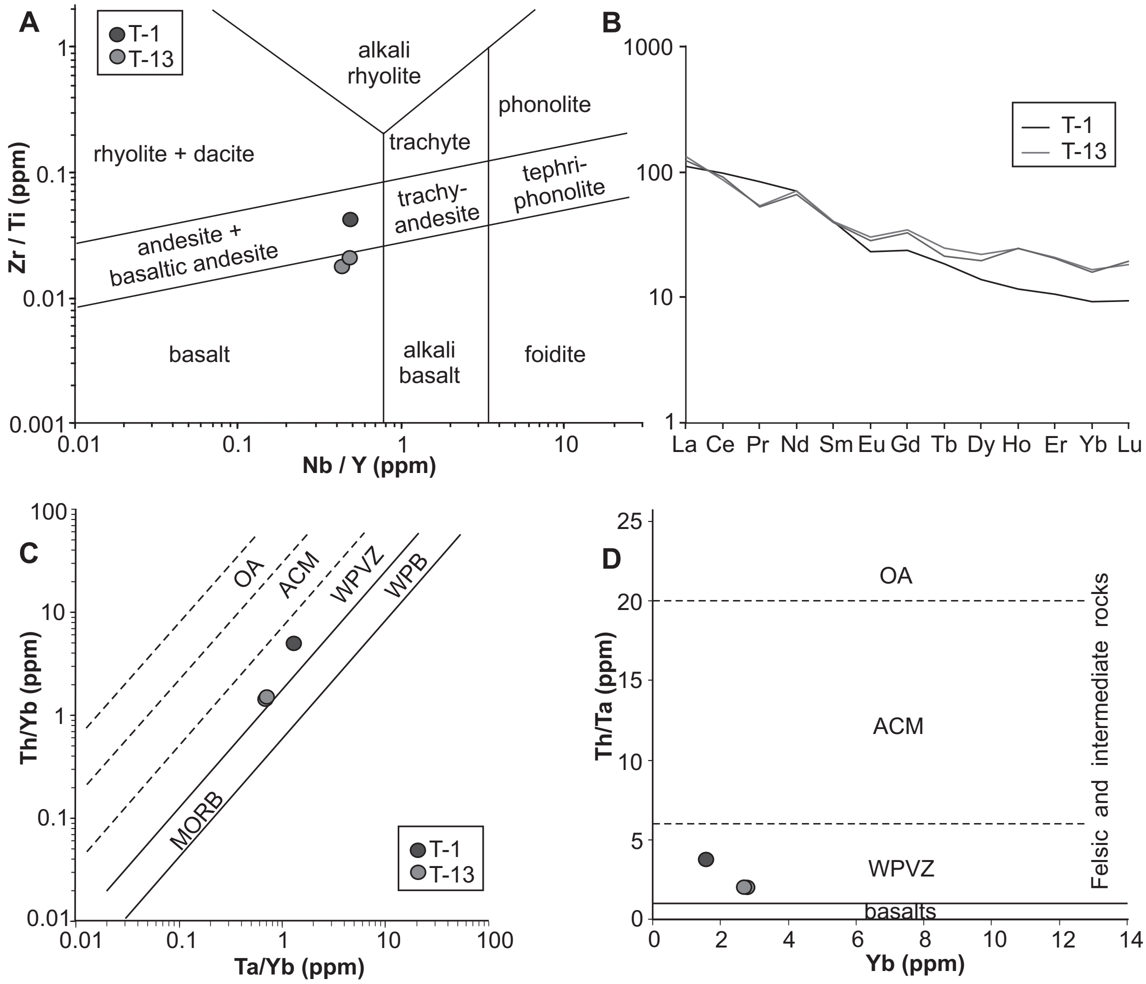

Fig. 2. A — Classification of the Tribeč Permian volcanic rocks based on Zr/Ti vs Nb/Y after Winchester & Floyd (1977) revised by Pearce (1996); **B** — Chondrite-normalized REE distribution of the studied pyroclastic rocks. Chondrite normalizing values after Sun & McDonough (1989); **C** — Th/Yb vs Ta/Yb discriminant diagram (after Pearce 1983) for the tectonic interpretation, revised by Gorton & Schandl (2000); **D** — Th/Ta vs Yb discrimination diagram for the tectonic interpretation after Gorton & Schandl (2000).

Detrital micas are present in amounts up to 3 % and based on the micas' chemical composition they belong to the true white micas (after Tischendorf et al. 2007; Supplementary Table S3). Two groups of white micas have been distinguished among them. The first group corresponds to the true muscovite with Si about 3.1 *apfu*. in the tetrahedral T site and low amount of Fe and Mg in octahedral M site. The second group is linked to the muscovite-celadonite series, containing a higher amount of tetrahedral co-ordinated Si, in the range from 3.3 to 3.6 *apfu*., as well as a high amount of Mg and Fe in the octahedral M site (Supplementary Table S3 and Fig. S1).

Primary fine-grained sedimentary matrix is completely recrystallized with significant preferred orientation. It consists of crystalline aggregate of quartz, sericite, Fe–Ti oxides and sporadically albite, chlorite and calcite. Zircon, apatite and opaque minerals (hematite, magnetite, Ti-magnetite) are common accessories. Monazite was identified rarely.

Results of zircon dating

Volcanic rocks

The magmatic zircon age data was acquired from the samples *T-1* and *T-2* (Fig. 1). A characteristic feature, of the both samples, is a high occurrence of inherited grains, which are mantled with newly formed igneous rims on their edges (Fig. 3A). Zircon ages, obtained from 14 grain edges wide enough to allow the measurements, gave a Concordia age of 263.1±2.6 Ma (Fig. 4). This age clearly corresponds to Guadalupian, just from the boundary Wordian/Capitanian and Capitanian Stage, and represents the magma crystallization age of the Tribeč Permian volcanic rocks. Only one solitary zircon grain in the sample *T-2* documents the Cisuralian age (Sakmarian–Artinskian, 291.6±3.3 Ma). This age probably indicates the older Permian magmatic event in the former sedimentary basin or in its wider surroundings. The magmatic

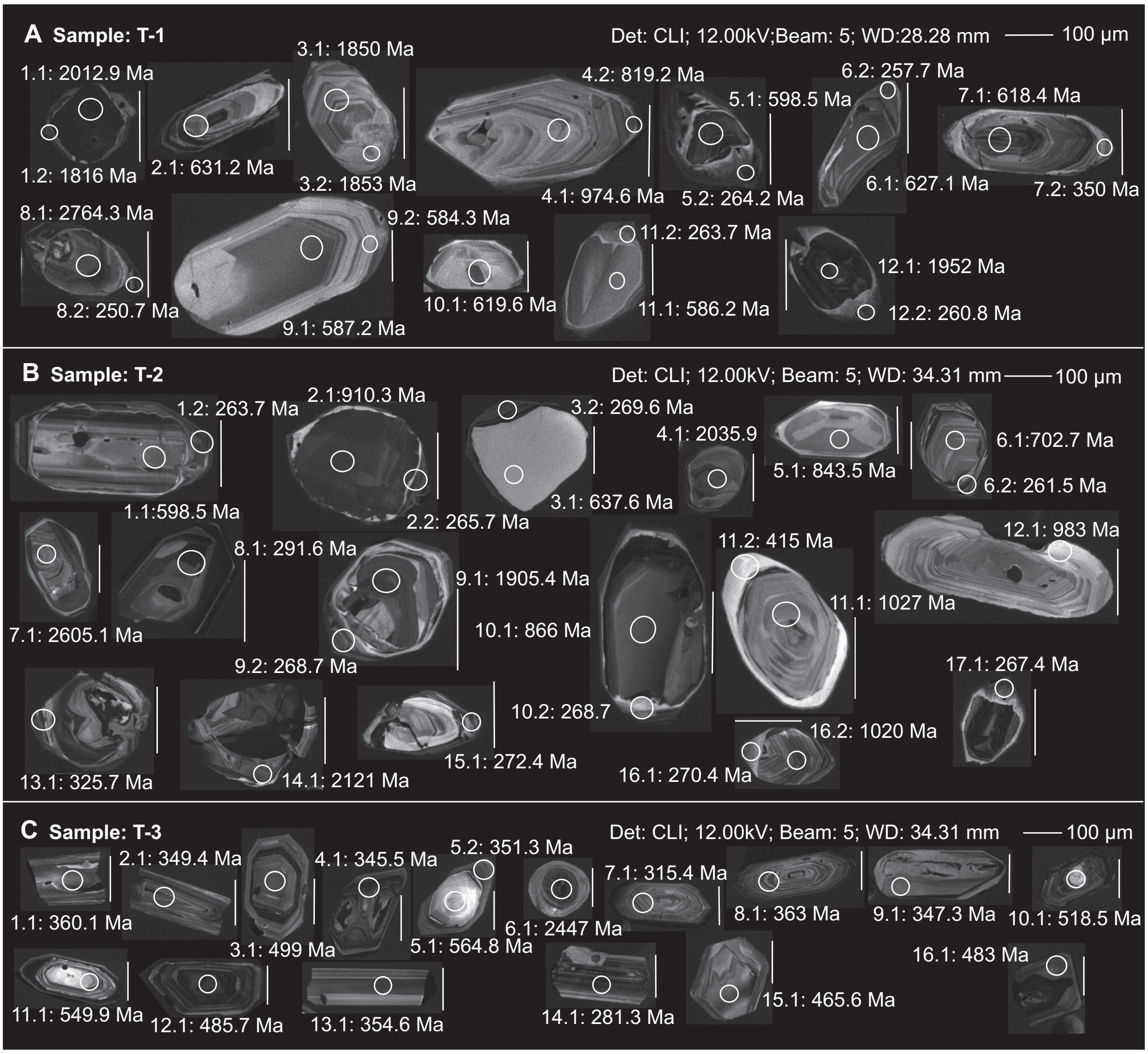

Fig. 3. Cathodoluminescence zircon images with indication of the age data (in Ma). The age data correspond to $^{238}U/^{206}Pb$ ages up to 1.0 Ga and to $^{206}Pb/^{207}Pb$ age data for >1.0 Ga. **A** — sample *T-1*; **B** — sample *T-2*; **C** — sample T-3.

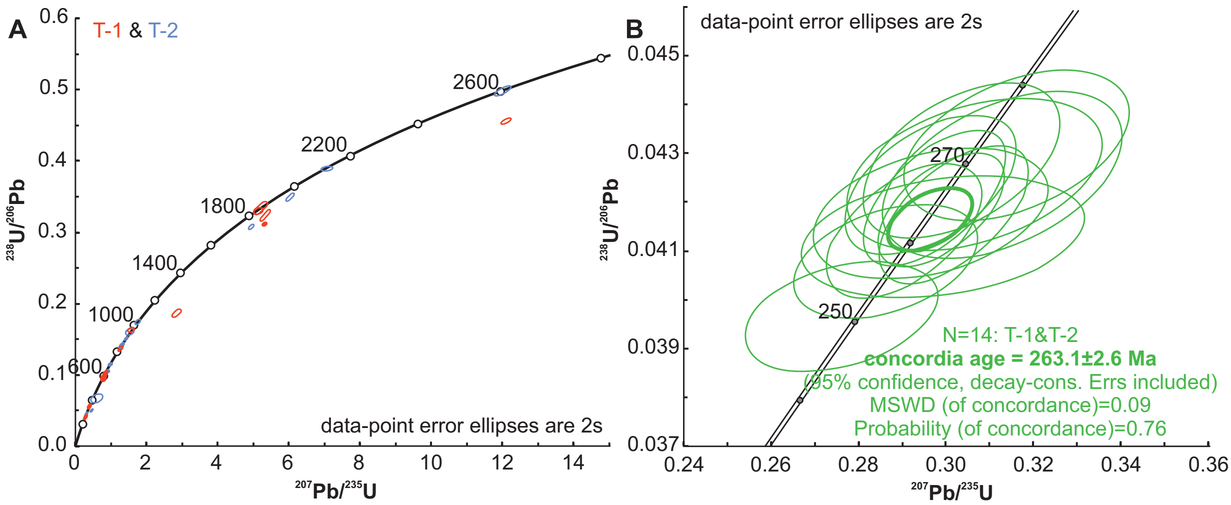

Fig. 4. Concordia plots of magmatic zircons from the *T-1* and *T-2* samples. **A** — Concordia plot for all magmatic and inherited zircons; **B** — selected sector of the Concordia for age spectrum from 250 to 280 Ma showing the Concordia age of the Tribeč volcanic rocks.

origin of the whole Permian population is confirmed by the $^{232}Th/^{238}U$ ratio values ranging from 0.12 to 0.44 (Wang et al. 2011) and the oscillatory growth zoning, as well as resorption discontinuities between magmatic rims and inherited cores.

Among inherited grains in the sample *T-1* (Table 2; Fig. 3) the Ediacaran ages are dominant, ranging from 586.2±7.9 to 627.1±2.8 Ma. The zircon analyses yielded U contents of 130–679 ppm and Th contents of 82–508 ppm. $^{232}Th/^{238}U$ ratios of the Ediacaran inherited zircons vary from 0.45 to 1.27, indicating a crystallization from felsic to intermediate igneous melt (Table 2). A further two inherited grains are considerably older, 2764.3±5.4 and 1952.0±8.6 Ma, with 0.73 and 1.67 $^{232}Th/^{238}U$ ratios, respectively. In one case, the inherited grain of 618.4±2.8 Ma is coated with the newly formed zircon 350.0±4.4 Ma old (spots 7.1 and 7.2; Table 2; Fig. 3). That could mean a partial melting and reworking of Cadomian crust in the early Variscan magma cycle.

Only one xenocrystic grain revealed the Tonian ages from 974.6±7.3 to 819.0±8.9 Ma (core → rim), showing well preserved growth oscillatory zoning, as well as the magmatic 0.81 and 0.77 $^{232}Th/^{238}U$ ratios (Table 2). The next two xenocrysts revealed 1850±15 and 2013±6 Ma ages in the core, corresponding to Orosirian. First of them indicates an intermediate to mafic magmatic source with the internal oscillatory grown texture and relatively high $^{232}Th/^{238}U$ ratio (1.26). On the other hand, the second Paleoproterozoic grain shows a homogeneous internal texture with very low $^{232}Th/^{238}U$ ratio value (0.02), likely indicating a high-grade metamorphic source (Fig. 3; Table 2). It is mantled by the 1816±22 Ma rim of magmatic origin ($^{232}Th/^{238}U$=0.19), however with a high discordance. Nevertheless, it suggests that the older Paleoproterozoic metamorphic grain has been reworked in a new magmatic cycle.

The age spectrum of the inherited grains in the sample *T-2* is dominated by Neoproterozoic ages ranging between 591 and 999 Ma (Table 3). Two other inherited grains revealed ~1.0 Ga ages, just straddling the boundary between Tonian and Stenian (1027±21 and 1058±14 Ma). The additional grains show Paleoproterozoic–Neoarchean ages. Three of them are around 2.0 Ga old (1905±8, 2036±7 and 2121±15 Ma) and one other corresponds

Table 2: U–Pb (SHRIMP) magmatic and detrital zircon age data (sample *T-1*).

Spot	$^{206}Pb_c$	U	Th	$^{232}Th/^{238}U$	$^{206}Pb^*$	(1)Age $^{206}Pb/^{238}U$	±	(1)Age $^{207}Pb/^{206}Pb$	±	Disc.	(1)Age $^{207}Pb/^{235}U$	±	Disc.	(1) $^{238}U/^{206}Pb^*$	%	(1) $^{207}Pb^*/^{206}Pb^*$	%	(1) $^{207}Pb^*/^{235}U$	%	(1) $^{206}Pb^*/^{238}U$	%	err corr
	%	ppm	ppm		ppm					%			%									
1.1	0.04	1151.61	24.52	0.02	311.00	1762.7	5.0	2012.9	5.9	14	1880.24	3.94	6.67	3.180	0.320	0.124	0.330	5.371	0.460	0.315	0.320	0.700
2.1	0.19	282.71	142.56	0.52	25.00	631.2	3.5	638.0	37.0	1	632.30	8.47	0.17	9.720	0.580	0.061	1.700	0.864	1.800	0.103	0.580	0.316
3.1	0.05	143.46	175.47	1.26	40.40	1828.0	10.0	1850.0	15.0	1	1838.27	8.50	0.56	3.050	0.630	0.113	0.830	5.113	1.000	0.328	0.630	0.608
4.1	0.21	113.31	89.36	0.81	15.90	974.6	7.3	931.0	45.0	−5	961.19	14.30	−1.38	6.126	0.810	0.070	2.200	1.577	2.300	0.163	0.810	0.343
5.1	0.19	674.58	293.06	0.45	56.50	598.5	2.3	555.0	30.0	−7	589.47	6.71	−1.51	10.278	0.400	0.059	1.400	0.787	1.500	0.097	0.400	0.279
6.1	0.10	411.69	507.95	1.27	36.20	627.1	2.9	591.0	27.0	−6	619.15	6.03	−1.27	9.787	0.490	0.060	1.200	0.840	1.300	0.102	0.490	0.369
7.1	0.14	463.15	220.42	0.49	40.10	618.4	2.8	599.0	28.0	−3	614.17	6.45	−0.68	9.932	0.470	0.060	1.300	0.831	1.400	0.101	0.470	0.338
8.1	0.06	456.11	323.29	0.73	178.00	2408.1	8.4	2764.3	5.4	15	2606.36	4.97	8.23	2.208	0.420	0.193	0.330	12.025	0.530	0.453	0.420	0.782
9.1	0.18	281.85	400.00	1.47	23.10	587.2	3.7	561.0	36.0	−5	581.48	7.97	−0.97	10.486	0.660	0.059	1.700	0.773	1.800	0.095	0.660	0.372
10.1	0.25	299.01	101.52	0.35	26.00	619.6	3.4	591.0	43.0	−5	613.61	9.67	−0.97	9.911	0.570	0.060	2.000	0.830	2.100	0.101	0.570	0.275
1.2	0.34	1026.49	186.52	0.19	168.00	1120.0	17.0	1816.0	22.0	62	1382.95	15.11	23.48	5.271	1.600	0.111	1.200	2.904	2.000	0.190	1.600	0.803
3.2	0.10	129.48	128.33	1.02	37.30	1864.0	20.0	1853.0	18.0	−1	1858.66	13.65	−0.29	2.983	1.200	0.113	1.000	5.237	1.600	0.335	1.200	0.778
4.2	0.49	369.68	274.47	0.77	43.20	819.2	8.9	874.0	37.0	7	834.18	11.95	1.83	7.380	1.200	0.068	1.800	1.274	2.100	0.136	1.200	0.548
5.2	0.07	843.07	138.25	0.17	30.30	264.2	2.9	277.0	37.0	5	265.46	4.67	0.48	23.900	1.100	0.052	1.600	0.299	2.000	0.042	1.100	0.573
6.2	0.36	628.17	166.27	0.27	22.10	257.7	2.9	236.0	64.0	−8	255.56	6.78	−0.83	24.520	1.200	0.051	2.800	0.286	3.000	0.041	1.200	0.388
7.2	0.40	231.37	54.20	0.24	11.10	350.0	4.4	327.0	90.0	−7	346.71	12.05	−0.94	17.920	1.300	0.053	3.900	0.407	4.100	0.056	1.300	0.309
8.2	0.78	1084.38	463.88	0.44	37.20	250.7	2.8	217.0	71.0	−13	247.48	7.25	−1.28	25.220	1.200	0.051	3.000	0.276	3.300	0.040	1.200	0.354
9.2	0.22	88.20	82.57	0.97	7.21	584.3	8.7	649.0	73.0	11	597.96	16.73	2.34	10.540	1.600	0.061	3.400	0.802	3.700	0.095	1.600	0.415
11.1	0.29	130.48	82.17	0.65	10.70	586.2	7.9	581.0	67.0	−1	584.91	15.12	−0.22	10.510	1.400	0.059	3.100	0.779	3.400	0.095	1.400	0.416
11.2	0.20	227.61	36.42	0.17	8.18	263.7	3.4	263.0	79.0	0	263.27	8.58	−0.16	23.950	1.300	0.052	3.500	0.296	3.700	0.042	1.300	0.356
12.1	0.06	499.15	807.71	1.67	137.00	1783.0	18.0	1952.0	8.6	9	1862.56	10.24	4.46	3.138	1.100	0.120	0.480	5.261	1.200	0.319	1.100	0.920
12.2	0.73	416.25	118.46	0.29	14.90	260.8	3.2	310.0	96.0	19	265.62	10.29	1.85	24.220	1.200	0.053	4.200	0.299	4.400	0.041	1.200	0.280

Errors are 1-sigma; Pb_c and Pb* indicate the common and radiogenic portions, respectively. (1) Common Pb corrected using measured ^{204}Pb. Error in Standard calibration was 0.45 % (black) and 0.37 % (gray – not included in above errors but required when comparing data from different mounts).

to Neoarchean (2605±14 Ma). The majority of analysed inherited cores, specify an acid magmatic provenance which is indicated by the $^{232}Th/^{238}U$ values, ranging from 0.13 to 0.87. These inherited cores exposed relatively well-preserved growth zoning with features of local recrystallization. From the measured inherited grains only two of them revealed low $^{232}Th/^{238}U$ values, corresponding to 0.06 and 0.08 (spots 2.1 and 14.1; Table 3), indicating a possible metamorphic origin (910.2±9.5 and 2121±15 Ma). The grains show a high complexity of their internal texture, with convolute and chaotic patchy domains.

Sedimentary rocks

17 analytical spots have been obtained on 16 detrital zircon grains from the sample *T-3* (Table 4). One analytical point was omitted from the calculation because of 26 % discordance. The sample *T-3* yielded concordant ages, mainly between 345±4 Ma and 565±7 Ma. The results are dominated by Tournaisian–Famennian ages, ranging from 342 to 367 Ma (8 spots). This set of analyses has been made from both, core as well as rim domains and gave the Concordia age of 352.4±2.9 Ma (Fig. 5). The concentration of U and Th is low to moderate, 281–1027 and 41–461 ppm, respectively. The $^{232}Th/^{238}U$ ratio values are varying between 0.12 and 0.99. A typical feature of the studied Tournaisian–Famennian zircons is the presence of well-developed growth oscillatory zoning (Fig. 3). They are most likely to be a result of crystallization from felsic melt composition (Wang et al. 2011). The only exception is the spot 5.2 (351.3±4 Ma), which overgrows the Ediacaran inherited grain (564.8±7.1 Ma), with low 0.06 $^{232}Th/^{238}U$ ratio value (Table 4; Fig. 3). The resorption interval with textural discontinuity has been observed, along which the original zoning is resorbed, and succeeded

Table 3: U–Pb (SHRIMP) magmatic and detrital zircon age data (sample *T-2*).

Spot	$^{206}Pb_c$ %	U ppm	Th ppm	$^{232}Th/^{238}U$	$^{206}Pb^*$ ppm	(1)Age $^{206}Pb/^{238}U$	±	(1)Age $^{207}Pb/^{206}Pb$	±	Disc. %	(1)Age $^{207}Pb/^{235}U$	±	Disc. %	(1) $^{238}U/^{206}Pb^*$	%	(1) $^{207}Pb^*/^{206}Pb^*$	%	(1) $^{207}Pb^*/^{235}U$	%	(1) $^{206}Pb^*/^{238}U$	%	err corr
1.1	0.14	310.43	121.79	0.41	26.00	598.5	6.9	601.0	31.0	0	599.08	8.60	0.10	10.280	1.200	0.060	1.500	0.804	1.900	0.097	1.200	0.640
2.1	0.06	612.85	37.27	0.06	79.90	910.3	9.5	899.0	16.0	−1	906.97	8.40	−0.37	6.594	1.100	0.069	0.780	1.443	1.400	0.152	1.100	0.822
3.1	0.13	89.99	11.13	0.13	8.05	637.6	8.2	667.0	52.0	5	644.22	13.36	1.04	9.620	1.400	0.062	2.400	0.886	2.800	0.104	1.400	0.485
3.2	0.04	728.88	91.57	0.13	26.80	269.6	3.1	287.0	31.0	7	271.39	4.29	0.66	23.410	1.200	0.052	1.400	0.306	1.800	0.043	1.200	0.647
4.1	0.05	480.39	187.66	0.40	144.00	1925.0	19.0	2035.9	7.1	6	1979.03	10.45	2.81	2.873	1.100	0.126	0.400	6.022	1.200	0.348	1.100	0.941
5.1	0.17	219.87	146.52	0.69	26.50	843.5	9.4	828.0	28.0	−2	839.52	10.28	−0.47	7.153	1.200	0.067	1.400	1.286	1.800	0.140	1.200	0.656
6.1	0.06	241.33	127.40	0.55	23.90	702.7	78.9	695.0	29.0	−1	700.76	9.11	−0.28	8.680	1.200	0.063	1.400	0.994	1.800	0.115	1.200	0.655
7.1	0.02	161.26	93.05	0.60	69.00	2605.0	25.0	2605.1	8.1	0	2605.19	12.19	0.01	2.008	1.200	0.175	0.480	12.010	1.300	0.498	1.200	0.923
8.1	0.00	801.97	90.79	0.12	31.90	291.6	3.3	289.0	26.0	−1	291.32	4.05	−0.10	21.610	1.200	0.052	1.100	0.332	1.600	0.046	1.200	0.717
9.1	0.02	484.82	99.61	0.21	129.00	1742.0	21.0	1905.4	8.1	9	1817.46	11.85	4.33	3.224	1.400	0.117	0.450	4.989	1.400	0.310	1.400	0.949
10.1	0.04	299.95	94.88	0.33	37.10	866.0	9.3	864.0	21.0	0	865.40	8.74	−0.07	6.955	1.200	0.068	1.000	1.345	1.500	0.144	1.200	0.755
11.1	0.06	217.86	156.20	0.74	32.50	1033.0	11.0	1027.0	21.0	−1	1031.22	10.36	−0.17	5.754	1.200	0.073	1.000	1.761	1.600	0.174	1.200	0.750
1.2	0.00	754.03	166.96	0.23	27.00	263.7	3.6	304.0	42.0	15	267.73	5.41	1.53	23.950	1.400	0.052	1.800	0.302	2.300	0.042	1.400	0.599
2.2	0.06	916.98	131.41	0.15	33.20	265.7	3.5	252.0	41.0	−5	264.37	5.12	−0.50	23.770	1.400	0.051	1.800	0.297	2.200	0.042	1.400	0.606
6.2	0.11	972.14	357.70	0.38	34.60	261.5	3.5	235.0	49.0	−10	258.87	5.71	−1.00	24.150	1.400	0.051	2.100	0.290	2.500	0.041	1.400	0.543
9.2	0.23	446.24	94.65	0.22	16.40	268.7	3.9	295.0	82.0	10	271.08	9.28	0.88	23.490	1.500	0.052	3.600	0.306	3.900	0.043	1.500	0.383
10.2	0.00	246.02	46.21	0.19	8.99	268.7	4.3	343.0	72.0	28	276.50	8.72	2.90	23.500	1.600	0.053	3.200	0.313	3.600	0.043	1.600	0.459
11.2	0.00	14.47	0.15	0.01	0.83	415.0	17.0	813.0	220.0	96	481.67	42.20	16.06	15.030	4.200	0.066	10.000	0.607	11.000	0.067	4.200	0.375
12.1	0.23	83.66	70.56	0.87	11.90	983.0	16.0	915.0	62.0	−7	961.98	21.76	−2.14	6.070	1.700	0.070	3.000	1.579	3.500	0.165	1.700	0.492
13.1	0.42	529.83	94.87	0.19	23.70	325.7	4.6	866.0	65.0	166	401.50	11.28	23.27	19.300	1.400	0.068	3.100	0.485	3.400	0.052	1.400	0.418
14.1	0.01	817.17	61.23	0.08	275.00	2134.0	23.0	2121.0	15.0	−1	2127.80	14.25	−0.29	2.549	1.300	0.132	0.880	7.130	1.600	0.392	1.300	0.827
15.1	0.19	530.63	115.66	0.23	19.70	272.4	3.9	334.0	68.0	23	278.82	8.05	2.36	23.170	1.500	0.053	3.000	0.316	3.300	0.043	1.500	0.437
16.1	0.00	368.61	42.41	0.12	13.60	270.4	4.0	258.0	61.0	−5	269.13	7.33	−0.47	23.340	1.500	0.051	2.700	0.304	3.100	0.043	1.500	0.495
16.2	0.13	267.37	188.20	0.73	41.00	1058.0	14.0	1020.0	31.0	−4	1045.82	13.71	−1.15	5.606	1.400	0.073	1.500	1.801	2.100	0.178	1.400	0.684
17.1	0.07	784.33	156.16	0.21	28.60	267.4	3.6	231.0	54.0	−14	263.74	6.27	−1.37	23.610	1.400	0.051	2.300	0.297	2.700	0.042	1.400	0.509

Errors are 1-sigma; Pbc and Pb* indicate the common and radiogenic portions, respectively. (1) Common Pb corrected using measured 204Pb. Error in Standard calibration was 0.41 % (black) and 0.56 % (gray – not included in above errors but required when comparing data from different mounts).

by the newly grown zircon, thus indicating a strong post-magmatic or metamorphic recrystallization process (Corfu et al. 2003). The rim shows the irregular and patchy internal texture.

A less frequent detrital zircon population is characterized by two zircons of Ordovician age (465.6±5.3 and 483.0±5.3 Ma) and equally, two zircons of Cambrian ages (485.7±5.3 and 499.0±5.6 Ma). The $^{232}Th/^{238}U$ ratio values, less than 1, indicate crystallization from a felsic igneous melt (Table 4). Their internal textures are typical of growth oscillatory zoning. Next, two Ediacaran grains (564.8±7.1 and 545.9±7.3 Ma) appear in the form of the inherited grains, which are overgrown by oscillatory zoned rims. The $^{232}Th/^{238}U$ ratio values, 0.88 and 0.67, correspond with a crystallization from felsic melt composition. Only one zircon grain yielded Neoarchean (2447±16 Ma) age. It is well rounded and overgrown by a light rim of newly formed zircon that is also perfectly rounded at its surface (Fig. 3). This suggests a multiple recycling.

Discussion

Age determination of volcanic rocks

U–Pb zircon dating of the volcanic rocks from the Veporic Unit of the Tribeč Mts. proved the Guadalupian volcanic event, revealed from the 263.1±2.6 Ma Concordia zircon age. This fact does not correspond well with the zircon age data which were obtained from the Brusno Formation volcanic rocks of the Northern Veporic Unit in the Čierťaž Mts. and showed rather older ages, matching Kungurian. This was documented by the 273±6 and 279±4 Ma ages with the SHRIMP method (Vozárová et al. 2016) and 278±11 Ma age from volcanic rocks and by the conventional multi-grain analysis (Kotov et al. 1996) from the volcanic dyke complex. It should be noted that the Kungurian age is the most documented age within the Western Carpathians Permian volcanites. Nearly the same ages were found in the Permian volcanites of the Northern Gemeric Unit (278±11 Ma monazite age – Rojkovič & Konečný 2005; 272±7 and 275±4 Ma zircon SHRIMP ages – Vozárová et al. 2012), in the Southern Gemeric Unit (276±11 Ma monazite age – Vozárová et al. 2008; 273±3 and 275±3 Ma zircon SHRIMP ages – Vozárová et al. 2009), as well as in the Bučina Fm. of the Bôrka Nappe (273±2 Ma zircon SHRIMP age – Vozárová et al. 2019). The beginning of the Permian volcanic activity in the Western Carpathians was documented by the reworked Cisuralian magmatic zircons (298–293 Ma; Vozárová et al. 2018, 2019) within detrital zircon assemblages in the associated sediments.

However, the zircon ages from the Permian volcanites in Tribeč Mts. could be compared with age data obtained from the Permian volcanic rocks in Považský Inovec Mts. (266±2 and 262±2 Ma – Putiš et al. 2016; 260±1 Ma – Pelech et al. 2017), as well as from the Permian volcanites in the Muráň

Table 4: U–Pb (SHRIMP) magmatic and detrital zircon age data (sample *T-3*).

Spot	$^{206}Pb_c$	U	Th	$^{232}Th/^{238}U$	$^{206}Pb^*$	(1)Age $^{206}Pb/^{238}U$	±	(1)Age $^{207}Pb/^{206}Pb$	±	Disc.	(1)Age $^{207}Pb/^{235}U$	±	Disc.	(1) $^{238}U/^{206}Pb^*$	%	(1) $^{207}Pb^*/^{206}Pb^*$	%	(1) $^{207}Pb^*/^{235}U$	%	(1) $^{206}Pb^*/^{238}U$	%	err
	%	ppm	ppm		ppm					%			%									corr
1.1	0.07	281.11	247.02	0.91	13.90	360.1	4.2	340.0	53.0	−5	357.48	7.84	−0.73	17.410	1.200	0.053	2.300	0.422	2.600	0.057	1.200	0.463
2.1	0.06	338.20	112.81	0.34	16.20	349.4	4.1	371.0	37.0	6	352.25	5.95	0.82	17.960	1.200	0.054	1.700	0.415	2.000	0.056	1.200	0.585
3.1	0.00	391.18	246.96	0.65	27.00	499.0	5.6	493.0	26.0	−1	497.96	6.69	−0.21	12.430	1.200	0.057	1.200	0.633	1.700	0.080	1.200	0.699
4.1	0.04	1027.39	284.22	0.29	48.60	345.5	3.8	363.0	21.0	5	347.87	4.42	0.68	18.160	1.100	0.054	0.940	0.409	1.500	0.055	1.100	0.768
5.1	0.18	136.19	116.09	0.88	10.70	564.8	7.1	558.0	48.0	−1	563.57	11.25	−0.22	10.920	1.300	0.059	2.200	0.742	2.600	0.092	1.300	0.510
5.2	0.06	471.73	25.46	0.06	22.70	351.3	4.0	304.0	35.0	−13	345.12	5.56	−1.76	17.860	1.200	0.052	1.500	0.405	1.900	0.056	1.200	0.609
6.1	0.01	1197.45	497.86	0.43	448.00	2329.0	22.0	2447.0	16.0	5	2392.37	12.87	2.72	2.298	1.100	0.159	0.920	9.550	1.400	0.435	1.100	0.769
7.1	0.06	398.76	177.54	0.46	19.20	351.4	4.0	323.0	39.0	−8	347.65	6.18	−1.07	17.850	1.200	0.053	1.700	0.408	2.100	0.056	1.200	0.570
8.1	0.11	367.62	41.36	0.12	18.30	363.0	4.3	353.0	41.0	−3	361.61	6.69	−0.38	17.260	1.200	0.054	1.800	0.428	2.200	0.058	1.200	0.556
9.1	0.12	310.99	44.46	0.15	14.80	347.3	4.0	386.0	41.0	11	352.47	6.55	1.49	18.070	1.200	0.054	1.800	0.415	2.200	0.055	1.200	0.547
10.1	11.87	132.59	56.86	0.44	10.80	518.5	9.9	382.0	380.0	−26	496.10	66.73	−4.32	11.940	2.000	0.054	17.000	0.630	17.000	0.084	2.000	0.118
11.1	0.15	100.19	64.53	0.67	7.62	545.9	7.3	538.0	58.0	−1	544.15	12.64	−0.32	11.320	1.400	0.058	2.600	0.709	3.000	0.088	1.400	0.465
12.1	0.00	690.45	135.28	0.20	46.40	485.7	5.3	503.0	19.0	4	488.78	5.43	0.63	12.780	1.100	0.057	0.880	0.618	1.400	0.078	1.100	0.787
13.1	0.08	481.46	461.07	0.99	23.40	354.6	4.1	344.0	32.0	−3	353.26	5.37	−0.38	17.680	1.200	0.053	1.400	0.416	1.800	0.057	1.200	0.641
14.1	1.75	976.18	717.76	0.76	38.10	281.3	3.1	295.0	63.0	5	282.83	7.41	0.54	22.420	1.100	0.052	2.800	0.321	3.000	0.045	1.100	0.380
15.1	0.13	518.40	202.18	0.40	33.40	465.6	5.3	422.0	92.0	−9	458.01	15.86	−1.63	13.350	1.200	0.055	4.100	0.570	4.300	0.075	1.200	0.272
16.1	0.10	596.69	160.96	0.28	39.90	483.0	5.3	461.0	26.0	−5	479.14	6.11	−0.80	12.850	1.100	0.056	1.200	0.603	1.600	0.078	1.100	0.701

Errors are 1-sigma; Pb_c and Pb* indicate the common and radiogenic portions, respectively. (1) Common Pb corrected using measured ^{204}Pb. Error in Standard calibration was 0.41 % (not included in above errors but required when comparing data from different mounts).

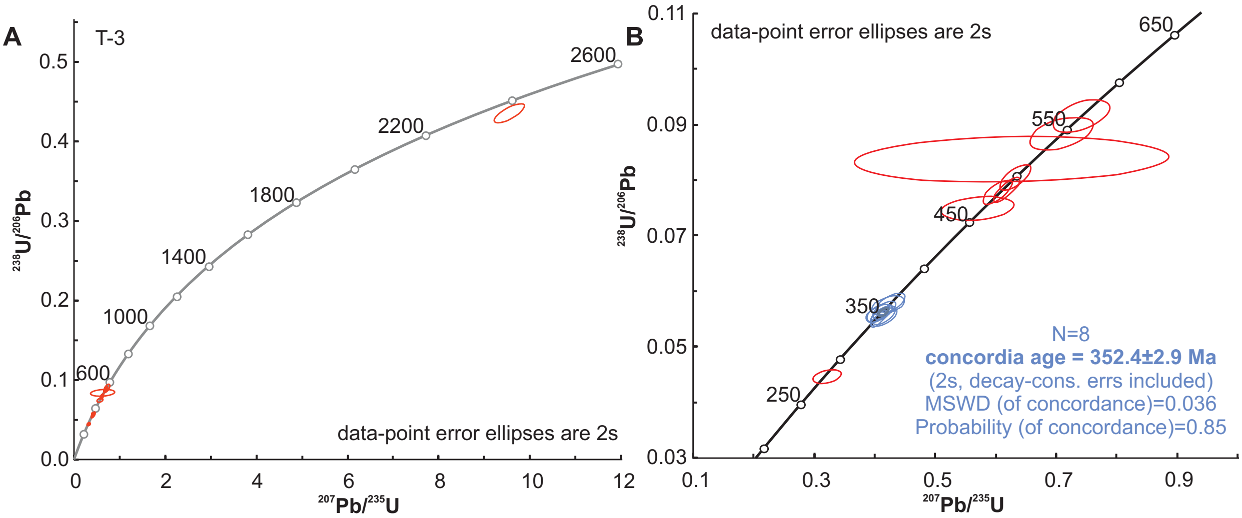

Fig. 5. Concordia plots of detrital zircons dated from the sample *T-3*. **A** — Concordia plot for all detrital zircons; **B** — selected sector of the Concordia for age spectrum from 250 to 550 Ma, showing Concordia age of the prominent cluster.

Nappe (263±2–269±2 Ma – Ondrejka et al. 2018) and from the Jasov Formation of the Bôrka Nappe (266±2 Ma – Vozárová et al. 2012). All these ages indicate the Guadalupian volcanic event, overwhelming mainly the Wordian and Capitanian Stages.

The obtained zircon age data confirm the multistage post-orogenic extensional tectonic regime for the genesis of the Permian volcanism in the Western Carpathians. It continued up to the Lopingian/Lower Triassic in some places, as is documented by the Re–Os molybdenite ages (257±3 and 256±4 Ma, Kohút et al. 2013) and zircon SHRIMP age (251±4 Ma, Vozárová et al. 2015) from the Northern Gemeric Unit.

Chemical composition data from the Tribeč Permian volcanic rocks suggest a within plate tectonic setting (Fig. 2c,d). The analysed volcanic rocks are characterized by a relatively high content of old xenocrystic zircon grains, which have been mantled by the newly formed zircons. The Permian magma was presumably a result of a partial melting of the mantle derived mafic magmatic source and along with a high assimilation of crustal material. Thus, the old xenocrystic zircon grains could entrain into this magma. The studied volcanic rocks are metaluminous and due to the low Zr saturation level of such magmas (Watson & Harrison 1983; Boehnke et al. 2013), the xenocrystic zircon grains survive. The melt was probably dry and cool.

Detrital zircon assemblage and xenocrystic grains

The detrital zircon population in the *T-3* sample together with the xenocrystic grains inherited in the volcanic rocks is dominated by the Tournaisian and Ediacaran zircon ages (Fig. 6). Lesser amounts of zircon ages correspond to the Cambrian–Ordovician and Tonian. Compared to this, the occurrence of the Paleoproterozoic/Neoarchean zircons is negligible.

We are aware that the stated number of age measurements of detrital zircons is too low for any interpretation of provenance. Since the detrital zircons were separated from a sample from the direct bedrock of the volcanic horizon, we allowed ourselves to evaluate them together with the xenocrystic grains. Both detrital and xenocrystic zircons have almost identical age peaks on the Kernel Density Estimation distribution curve. The only difference is the absence of Cambrian–Ordovician ages between xenocrystic grains. Of course, this is perhaps due to the smaller number of grains measured. Even so, we assumed the same crustal source, although of course the volcanics reflect a much deeper horizon extending into the mantle.

The zircon age distribution, shown by the Kernel Density Estimation (KDE), identify the main peaks at the 353 and 618 Ma and further small peaks at the 484, 847, 1000 and 1855 Ma (Fig. 6). The presented detrital zircon ages specify, generally, the provenance of the Tribeč Permian deposits from the Western Carpathian Crystalline Basement (WCCB). A similar association of xenocrystic zircon grains was assimilated by the Permian magma and represents the same crustal source.

The Devonian/Mississippian I-type granitoids were determined by the SIMS U–Pb zircon method in the crystalline basement of the Tribeč Mts. (367–358 Ma; Broska et al. 2013). Here, the authors also described the Ordovician and Archean inherited zircon grains.

Similarly, in other areas of the Western Carpathian Tatric and Veporic crystalline basement comparable ages of I- and S-type granitoids were found. Data demonstrate ages between 367–353 Ma (e.g., zircon data – Kohút et al. 2008, 2009; Burda et al. 2011; Vozárová et al. 2016; monazite chemical data – Finger et al. 2003; Petrík & Konečný 2009). Consistently, the previous ID-TIMS multigrain zircon analysis (Bibikova et al. 1988; Shcherbak et al. 1990) and single grain evaporation ages (Kráľ et al. 1997; Poller & Todt 2000; Gaab et al. 2005)

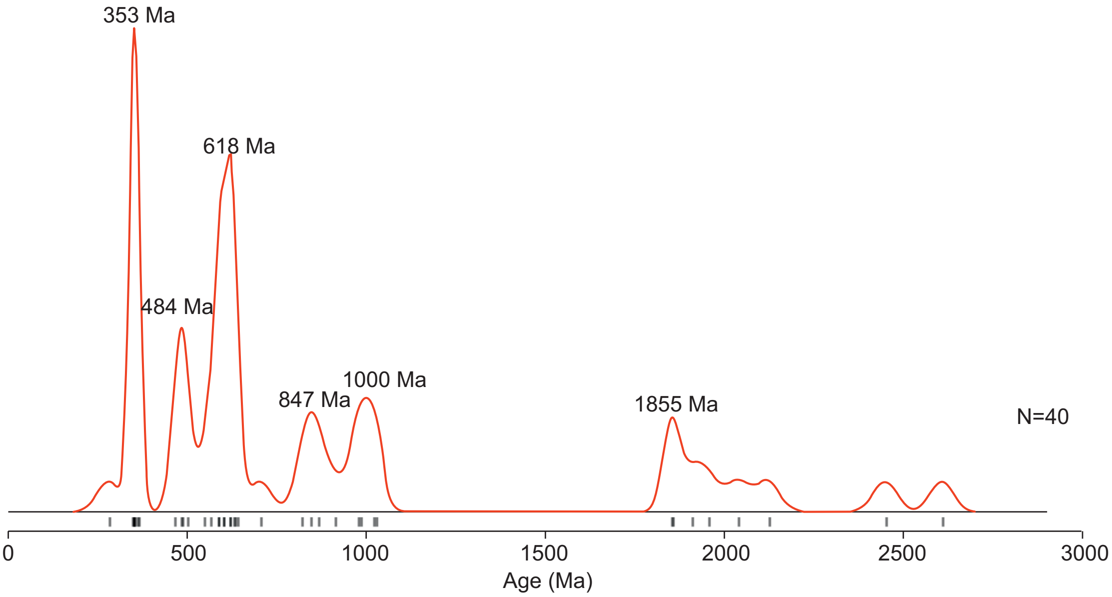

Fig. 6. Kernel Density Estimation for the entire detrital zircon population and xenocrystic grains from the volcanic rocks, with discordant filter of 10 %.

specify nearly synchronous magmatic events in the range of 345–356 Ma. SIMS zircon dating from the WCCB high-grade orthogneisses yielded nearly identical ages (371–363 Ma SHRIMP data, Putiš et al. 2008, 2009; 357–363 Ma single grain evaporation ages, Poller et al. 2000; Putiš et al. 2003).

A smaller age cluster among the Tribeč Permian detrital zircon assemblage is represented by the Cambrian–Ordovician ages spanning 499–466 Ma. These ages have been defined in layered amphibolites and orthogneisses of the WCCB Tatric and Veporic units (SHRIMP zircon data Putiš et al. 2008, 2009; single grain evaporation Gaab et al. 2005; chemical monazite ages Janák et al. 2002). The second largest group of detrital zircons ages correspond to the Ediacaran in the range of 546–631 Ma, with leading peak at 618 Ma (Fig. 6). A smaller number of detrital zircons are represented by the Tonian ages, giving two small sub-peaks at 847 and 1000 Ma on the KDE distribution curve (Fig. 6). The Paleoproterozoic/Neoarchean detrital zircons of the 1.8–2.0 Ga and 2.4–2.7 Ga are negligible (Table 1) and hold remarkable features of multiple recycling.

Generally, the presented Tribeč Permian detrital zircon assemblage, as well as the xenocrystic grains population from the associated volcanic rocks, indicate the provenance from the Variscan WCCB crust, with highly evolved detrital material from the earliest I-type Variscan granitoids. The studied detrital zircon population resembles the Ediacaran (546–631 Ma) and Paleoproterozoic–Neoarchean (1.8–2.8 Ga) zircon ages, which is usually taken to indicate a clear affinity with the peri-Gondwanan Cadomian Belt and the West African Craton provenance throughout the Neoproterozoic–Ordovician time (e.g., Fernández-Suárez et al. 2002; Friedl et al. 2004; Linnemann et al. 2007, 2014; Meinhold et al. 2010; Drost et al. 2011; Henderson et al. 2016; Avigad et al. 2018 and references therein).

Conclusions

- The obtained *in situ* U–Pb (SHRIMP) magmatic zircon ages clearly document the timing of the Mid-Permian lithospheric extension in the internal zone of the Variscan Western Carpathians. The Concordia age 263.1±2.6 Ma corresponds to the uppermost Guadaluppian (Capitanian) and represents the magma crystallization age of the Tribeč Permian volcanic rocks.
- Detrital zircon population from the Tribeč Permian metasediments as well as the xenocrystic grains from the associated volcanic rocks, show internal textures and Th/U ratios indicating magmatic sources as dominant. Metamorphic sources are considerably reduced. The dominant Mississippian and Ediacaran zircon ages allow us to assume their derivation from the Western Carpathian Crystalline Basement, with a high proportion of detritus from the Variscan I-type granitoids and from involved fragments of the Cadomian crust. The acquired detrital zircons assemblage enable us to correlate the source area of the Tribeč Permian sedimentary rocks with the equivalent provenances for the Tatricum, Northern Veporicum, as well as displaced Hronicum basement rocks.

Acknowledgements: The financial support of the Slovak Research and Development Agency (projects ID: APVV-0146-16) and of the Scientific Grant Agency of the Ministry of Education of the Slovak Republic and the Slovak Academy of Sciences (project VEGA 2/0006/19) is gratefully appreciated. The authors would like to thank J. Ulrych and unknown reviewer for constructive reviews and for their helpful and critical comments which led to significant improvement of an earlier version of the manuscript.

References

Andrusov D. 1968: Grundriss der Tektonik der Nördlichen Karpaten. *Publish. Slovak Acad. Sciences,* Bratislava, 1–188.

Avigad D., Rossi Ph., Gerdes A. & Abdo A. 2018: Cadomian metasediments and Ordovician sandstones from Corsica: detrital zircon U–Pb–Hf constraints on their provenance and paleogeography. *Int. J. Earth Sci. (Geol. Rundsch.)* 107, 2803–2818. https://doi.org/10.1007/s00531-018-1629-3

Bibikova E.V., Cambel B., Korikovsky S.P., Broska I., Gracheva T.V., Makarov V.A. & Arakeliants M.M. 1988: U–Pb and K–Ar isotopic dating of Sinec (Rimavica granites) (Kohút zone of Veporides). *Geol. Zborn. Geol. Carpath*. 39,147–157.

Biely A. 1974: Geological map of Tribeč Mts., 1:50.000. *Dionýz Štúr Inst. Geol*., Bratislava.

Biely A. 1977: "Gemericum" in the Tribeč Mts. *Geol. Práce Správy* 67, 163–168 (in Slovak).

Biely A., Bezák V., Elečko M., Gross P., Kaličiak M., Konečný V., Lexa J., Mello J., Nemčok J., Potfaj M., Rakús M., Vass D., Vozár J. & Vozárová A. 1996: Explanation to geological map of Slovakia, 1:500.000. *Dionýz Štúr Publishers*, Bratislava, 1–232 (in Slovak with English summary).

Biely A., Bujnovský A., Vozárová A., Klinec A., Miko O., Halouzka R., Vozár J., Beňuška P., Bezák V. et al. 1997: Explanation to Geological map of Nízke Tatry Mts., 1:50.000. *Geol. Surv. Slovak Rep., Dionýz Štúr Publishers,* Bratislava, 1–232.

Black L.P., Kamo S.L., Allen C.M., Aleinikoff J.N., Davis D.W., Korsch R.J. & Foudoulis C. 2003: TEMORA 1: a new zircon standard for Phanerozoic U–Pb geochronology. *Chem. Geol.* 200, 155–170. https://doi.org/10.1016/S0009-2541(03)00165-7

Boehnke P., Watson E.B., Trail D., Harrison T.M. & Schmitt A.K. 2013: Zircon saturation re-revisited. *Chem. Geol*. 351, 324–334. https://doi.org/10.1016/j.chemgeo.2013.05.028

Broska I., Petrík I., Be′eri-Shlevin Y., Majka J. & Bezák V. 2013: Devonian/Mississippian I-type granitoids in the Western Carpathians: A subduction-related hybrid magmatism. *Lithos* 162–163, 27–36. https://doi.org/10.1016/j.lithos.2012.12.014

Burda J., Gawęda A. & Klötzli U. 2011: Magma hybridization in the Western Tatra Mts. granitoid intrusion (S-Poland, Western Carpathians). *Miner. Petrol.* 103, 1, 19–36. https://doi.org/10.1007/s00710-011-0150-1

Corfu F., Hanchar J.M., Hoskin P.W.O. & Kinny P. 2003: Atlas of Zircon Textures. In: Hanchar J.M. & Hoskin P.W.O. (Eds.): Zircon. *Rev. Mineral. Geochem.* 53, *Mineralogical Society of America and Geochemical Society*, 469–500. https://doi.org/10.2113/0530469

Demko R. & Hraško Ľ. 2013: Rhyolite body Gregová near the Telgárt village (Slovakia). *Mineralia Slovaca* 45, 161–174 (in Slovak with English summary).

Drost K., Gerdes A., Jeffries T., Linnemann U. & Storey C. 2011: Provenance of Neoproterozoic and early Paleozoic siliciclastic rocks of the Teplá-Barrandian unit (Bohemian Massif): Evidence from U–Pb detrital zircon ages. *Gondwana Res.* 19, 1, 213–231. https://doi.org/10.1016/j.gr.2010.05.003

Ďurovič V., Korikovskij S.P., Laputina I.P. & Ďurovičová M. 1992: Propylitized basalts and plagiodacites from Permian metasediments of the Tribeč Mts. *Mineralia Slovaca* 24, 407–412 (in Slovak).

International Commission on Stratigraphy 2019: International Chronostratigraphic Chart v 2019/05

Finger F., Broska I., Haunschmid B., Hraško Ľ., Kohút M., Krenn E., Petrík I., Riegler G. & Uher P. 2003: Electron-microprobe dating of monazites from Western Carpathians basement granitoids: Plutonic evidence for an important Permian rifting event subsequent to Variscan crustal anatexis. *Int. J. Earth Sci. (Geol. Rundsch.)* 92, 86–98. https://doi.org/10.1007/s00531-002-0300-0

Fernández-Suárez J., Guttiérez-Alonso G. & Jeffries T.E. 2002: The importance of along-margin terrane transport in northern Gondwana: insights from detrital zircon parentage in Neoproterozoic rocks from Iberia and Brittany. *Earth Planet. Sci. Lett*. 204, 75–88. https://doi.org/10.1016/S0012-821X(02)00963-9

Friedl G., Finger F., Paquette J.L., von Quadt A., McNaughton N.J. & Fletcher I.R. 2004: Pre-Variscan geological events in the Austrian part of the Bohemian Massif deduced from U-Pb zircon ages. *Int. J. Earth Sci. (Geol. Rundsch.)* 93, 802–823. https://doi.org/10.1007/s00531-004-0420-9

Fusán O., Biely A., Ibrmajer J., Plančár J. & Rozložník L. 1987: Basement of the Tertiary Basins in the Inner West Carpathians. *Monogr., Dionýz Štúr Inst. Geol.*, Bratislava, 1–123 (in Slovak).

Gaab A.S., Poller U., Janák M., Kohút M. & Todt W. 2005: Zircon U–Pb geochronology and isotopic characterization for the pre-Mesozoic basement of the Northern Veporic Unit (Central Western Carpathians, Slovakia). *Schweiz. Mineral. Petrogr. Mitt*. 85, 69–88.

Gorton M.P. & Schandl E.S. 2000: From continents to island arcs: a geochemical index of tectonic setting for arc-related and within-plate felsic to intermediate volcanic rocks. *Can. Mineral.* 38, 1065–1073. https://doi.org/10.2113/gscanmin.38.5.1065

Henderson B.J., Collins W.J., Murphy J.B., Gutiérrez-Alonso G. & Hand M. 2016: Gondwanan basement terranes of the Variscan Appalachian orogen: Baltican, Saharan and West African hafnium isotopic fingerprints in Avalonia, Iberia and the Armorican Terranes. *Tectonophysics* 681, 278–304. https://doi.org/10.1016/j.tecto.2015.11.020

Hiess J., Condon D.J., McLean N. & Noble S.R. 2012: $^{238}U/^{235}U$ systematics in terrestrial uranium-bearing minerals. *Science* 335, 1610–1614. https://doi.org/10.1126/science.1215507

Ivanička J., Hók J., Polák M., Határ J., Vozár J., Nagy A., Fordinál K., Pristaš J., Konečný V., Šimon L., Kováčik M., Vozárová A., Fejdiová O., Marcin D., Liščák P., Macko A., Lanc J., Šantavý J. & Szalaiová V. 1998: Explanation to geological map of Tribeč Mts., 1.50.000. *Geol. Surv. Slovakia, Dionýz Štúr Publ*., 1–247 (in Slovak with Englich summary).

Janák M., Finger F., Plašienka D., Petrík I., Humer B., Méres Š. & Lupták B. 2002: Variscan high P-T recrystallization of Ordovician granitoids in the Veporic unit (Nízke Tatry Mountains, Western Carpathians): new petrological and geochronological data. *Geolines* 14, 38–39.

Kohút M., Poller U., Gurk C. & Todt W. 2008: Geochemistry and U–Pb detrital zircon ages of metasedimentary rocks of the Lower Unit, Western Tatra Mountains (Slovakia). *Acta Geol. Pol.* 58, 4, 371–384.

Kohút M., Uher P., Putiš M., Ondrejka M., Sergeev S., Larionov A. & Paderin I. 2009: SHRIMP U–Th–Pb zircon dating of the granitoid massifs in the Malé Karpaty Mountains (Western Carpathians): evidence of Meso-Hercynian successive S- to I-type granitic magmatism. *Geol. Carpath.* 60, 5, 345–350. https://doi.org/10.2478/v10096-009-0026-z

Kohút M., Trubač J., Novotný L., Ackerman L., Demko R., Bartalský B. & Erban V. 2013: Geology and Re-Os molybdenite geochronology of the Kurišková U–Mo deposit (Western Carpathians, Slovakia). *J. Geosci*. 58, 275–286. https://doi.org/10.3190/jgeosci.150

Kotov A.B., Miko O., Putiš M., Korikovsky S.P., Salnikova E.B., Kovach V.P., Yakovleva S., Bereznaya N.G., Kráľ J. & Krist E. 1996: U/Pb dating of zircons of postorogenic acid metavolcanics and metasubvolanics: a record of Permian-Triassic taphrogeny of the West-Carpathian basement. *Geol. Carpath*. 47, 73–79.

Kráľ J., Hess J.C., Kober B. & Lippolt H.J. 1997: $^{207}Pb/^{206}Pb$ and $^{40}Ar/^{39}Ar$ data from plutonic rocks of the Strážovské vrchy Mts. basement, Western Carpathians. In: Grecula P., Hovorka D. & Putiš M. (Eds.): Geological evolution of the Western Carpathians. *Miner. Slov. – Monograph*, Bratislava, 253–260.

Linnemann U., Gerdes A., Drost K. & Buschmann B. 2007: The continuum between Cadomian orogenesis and opening of the Rheic Ocean: constraints of the LA-ICP-MS zircon dating and analyses of plate-tectonic setting, Saxo-Thuringian zone, northeastern Bohemian Massif, Germany. *Geol. Soc. Amer. Spec. Pap*. 423, 61–96.

Linnemann U., Gerdes A., Hofmann M. & Marko L. 2014: The Cadomian Orogen: Neoproterozoic to Early Cambrian crustal growth and orogenic zoning along the periphery of the West African Craton – Constraints from U-Pb zircon ages and Hf isotopes (Schwarzburg Antiform, Germany). *Precambrian Res*. 244, 236–278. https://doi.org/10.1016/j.precamres.2013.08.007

Ludwig K.R. 2005: SQUID 1.12 A User's Manual. A Geochronological Toolkit for Microsoft Excel. *Berkeley Geochronology Centre Spec. Publ.,* 1–22. http://www.bgc.org/klprogrammenu.html

Ludwig K.R. 2012: User's Manual for Isoplot 3.75. A geochronological Toolkit for Microsoft Excel. *Berkeley Geochronology Centre Special Publication* No. 5, 1–71. http://www.bgc.org/isoplot.html

Maheľ M. 1986: Geological structure of the Czechoslovak Carpathians, Part 1: Paleoalpine units. *Veda Publ. House*, Bratislava, 1–503 (in Slovak).

MacLean W.H. & Barrett T.J. 1993: Lithogeochemical techniques using immobile elements. *J. Geochem. Explor*. 48, 109–133.

Meinhold G., Kostopoulos D., Frei D., Himmerkus F. & Reischmann T. 2010: U–Pb LA-SF-ICP-MS zircon geochronology of the Serbo–Macedonian Massif, Greece: paleotectonic constraints for Gondwana-derived terranes in the Eastern Mediterranean. *Int. J. Earth Sci. (Geol. Rundsch.)* 99, 913–832. https://doi.org/10.1007/s00531-009-0425-5

Nelson N.T. & Montana A. 1992: Sieve-plagioclase in volcanic rocks produced by rapid decompression. *Am. Mineral.* 77, 1242–1249.

Ondrejka M., Li X-H., Vojtko R., Putiš M., Uher P. & Sobocký T. 2018: Permian A-type rhyolites of the Muráň Nappe, Inner Western Carpathians, Slovakia: in-situ zircon U–Pb SIMS ages and tectonic setting. *Geol. Carpath.* 69, 2, 187–198. https://doi.org/10.1515/geoca-2018-0011

Pearce J.A. 1983: The role of sub-continental lithosphere in magma genesis of destructive plate margins. In: Hawkesworth C.J. & Norry M.J. (Eds.): Continental basalts and mantle xenoliths. *Shiva*, Nantwich, 230–249.

Pearce J.A. 1996: A user's guide to basalt discrimination diagrams. In: Wyman D.A. (Ed.): Trace element geochemistry of volcanic rocks: applications for massive sulphide exploration. *Geol. Assoc. Canada, Short Course Notes* 12, 79–113.

Pelech O., Vozárová A., Uher P., Petrík I., Plašienka D., Šarinová K. & Rodionov N. 2017: Late Permian volcanic dykes in the crystalline basement of the Považský Inovec Mts. (Western Carpathians): U–Th–Pb SHRIMP and monazite chemical dating. *Geol. Carpath*. 68, 6, 530–542. https://doi.org/10.1515/geoca-2017-0035

Petrík I. & Konečný P. 2009: Metasomatic replacement of inherited metamorphic monazite in a biotite-garnet granite from the Nízke Tatry Mountains, Western Carpathians, Slovakia: chemical dating and evidence for disequilibrium melting. *Am. Mineral*. 94, 957–974. https://doi.org/10.2138/am.2009.2992

Plašienka D. 2018: Continuity and episodicity in the early Alpine tectonic evolution of the Western Carpathians: How large-scale processes are expressed by the orogenic architecture and rock record data. *Tectonics* 37, 2029–2079. https://doi.org/10.1029/2017TC004779

Plašienka D., Grecula P., Putiš M., Kováč M. & Hovorka D. 1997: Evolution and structure of the Western Carpathians: an overview. In: Grecula P., Hovorka D., Putiš M. (Eds.): Geological evolution of the Western Carpathians. *Mineralia Slovaca, Monograph*, Bratislava, 1–24.

Poller U. & Todt W. 2000: U–Pb single zircon data of granitoids from the High Tatra Mountains (Slovakia): implications for the geodynamic evolution. *Geol. Soc. Am. Spec. Pap.* 350, 235–243.

Poller U., Janák M., Kohút M. & Todt W. 2000: Early Variscan magmatism in the Western Carpathians: U-Pb zircon data from granitoids and orthogneisses of the Tatra Mountains (Slovakia). *Int. J. Earth Sci. (Geol. Rundsch.)* 89, 2, 336–349. https://doi.org/10.1007/s005310000082

Putiš M., Kotov A. B., Petrík I., Korikovsky S. P., Madarás J., Salnikova E.B., Yakovleva S.Z., Berezhnaya N.G., Plotkina Y.V., Kovach V.P., Lupták B. & Majdán M. 2003: Early– vs. Late orogenic granitoids relationships in the Variscan basement of the Western Carpathians. *Geol. Carpath.* 54, 163–174.

Putiš M., Sergeev S., Ondrejka M., Larionov A., Siman P., Spišiak J., Uher P. & Paderin I. 2008: Cambrian–Ordovician metaigneous rocks associated with Cadomian fragments in the West-Carpathian basement dated by SHRIMP on zircons: a record from the Gondwana active margin setting. *Geol. Carpath*. 59, 1, 3–18.

Putiš M., Ivan P., Kohút M., Spišiak J., Siman P., Radvanec M., Uher P., Sergeev S., Larionov A., Méreš Š., Demko R. & Ondrejka M. 2009: Meta-igneous rocks of the West-Carpathian basement, Slovakia: indicators of Early Paleozoic extension and shortening events. *Bull. Soc. Géol. Fr.* 180, 6, 461–471.

Putiš M., Li J., Ružička P., Ling X. & Nemec O. 2016: U/Pb SIMS zircon dating of a rhyolite intercalation in Permian siliciclastics as well as a rhyodacite dyke in micaschists (Infratatricum, W. Carpathians). *Mineralia Slovaca* 48, 135–144.

Rakús M., Potfaj M. & Vozárová A. 1998: Basic paleogeographic and paleotectonic units of the Western Carpathians. In: Rakús M. (Ed.): Geodynamic development of the Western Carpathians. *Dionýz Štúr Publ.*, Bratislava, 5–26.

Rojkovič I. & Konečný P. 2005: Th–U–Pb dating of monazite from the Cretaceous uranium vein mineralization in the Permian rocks of the Western Carpathians. *Geol. Carpath.* 56, 493–502.

Shcherbak N.P., Cambel B., Bartnitsky E.N. & Stepanyuk L.M. 1990: U–Pb age of granitoid rock from the quarry Dubná Skala–Malá Fatra Mts. *Geol. Zborn. Geol. Carpath*. 41, 407–414.

Stewart M.L. & Pearce T.H. 2004: Sieve-textured plagioclase in dacitic magma: Interference imaging results. *Am. Mineral.* 89, 2–3, 348–351. https://doi.org/10.2138/am-2004-2-313

Steiger R.H. & Jäger E. 1977: Subcommission on geochronology: Convention on the use of decay constants in geo- and cosmochronology. *Earth Planet. Sci. Lett.* 36, 359–362.

Sun S.S. & McDonough W.F. 1989: Chemical and isotope systematic of oceanic basalts implications for mantle composition and processes. In: Sounders A.D. & Norry M.J. (Eds.): Magmatism in ocean basins. *Geol. Soc. London, Spec. Publ.* 42, 313–345.

Tischendorf G., Förster H.-J., Gottesmann B. & Rieder M. 2007: True and brittle micas: Composition and solid-solution series. *Mineral. Mag.* 71, 3, 285–320. https://doi.org/10.1180/minmag.2007.071.3.285

Tsuchiyama A. & Takahashi E. 1983: Melting kinetics of plagioclase feldspars. *Contrib. Mineral*. *Petrol.* 84, 4, 345–354.

Vermeesch P. 2018: IsoplotR: A free and open toolbox for geochronology. *Geosci. Frontiers* 9, 1479–1493. https://doi.org/10.1016/j.gsf.2018.04.001

Vozárová A. 1979: Lithofacial characteristics of Permian in NW part of Veporicum. *Západné Karpaty, Sér Min Petr Geoch Metalog* 6, 61–116 (in Slovak with English summary).

Vozárová A. & Vozár J. 1988: Late Paleozoic in West Carpathians. *Monogr., D. Štúr. Inst. Geol.*, Bratislava, 1–314.

Vozárová A., Konečný P., Vozár J. & Šmelko M. 2008: Upper Jurassic–Lower Cretaceous tectonothermal events in the Southern Gemeric Permian rocks deduced from electron microprobe dating of monazite. *Geol. Carpath*. 59, 2, 89–102.

Vozárová A., Šmelko M. & Paderin I. 2009: Permian single crystal U–Pb zircon age of the Rožňava Formation volcanites (Southern Gemeric Unit, Western Carpathians, Slovakia). *Geol. Carpath.* 60, 439–448. https://doi.org/10.2478/v10096-009-0032-1

Vozárová A., Šmelko M., Paderin I. & Larionov A. 2012: Permian volcanics in the Northern Gemericum and Bôrka Nappe system: U-Pb zircon dating and implication to geodynamic evolution (Western Carpathians, Slovakia). *Geol. Carpath.* 63, 191–200. https://doi.org/10.2478/v10096-012-0016-4

Vozárová A., Presnyakov S., Šarinová K. & Šmelko M. 2015: First evidence for Permian-Triassic boundary volcanism in the Northern Gemericum: geochemistry and U-Pb zircon geochronology. *Geol. Carpath.* 66, 5, 375–391. https://doi.org/10.1515/geoca-2015-0032

Vozárová A., Rodionov N., Vozár J., Lepekhina E. & Šarinová K. 2016: U–Pb zircon ages from Permian volcanic rocks and tonalite of the Northern Veporicum (Western Carpathians). *J. Geosci.* 61, 221–237. https://doi.org/10.3190/jgeosci.215

Vozárová A., Larionov A., Šarinová K., Vďačný M., Lepekhina E., Vozár J. & Lvov P. 2018: Detrital zircons from the Hronicum Carboniferous–Permian sandstones (Western Carpathians, Slovakia): depositional age and provenance. *Int. J. Earth Sci. (Geol. Rundsch.)* 107, 1539–1555. https://doi.org/10.1007/s00531-017-1556-8

Vozárová A., Šarinová K., Laurinc D., Lepekhina E., Vozár J., Rodionov N. & Lvov P. 2019: Exhumation history of the Variscan suture: constrains on the detrital zircon geochronology from Carboniferous–Permian sandstones (Northern Gemericum; Western Carpathians). *Geol. Carpath*. 70, 6, 512–530. https://doi.org/10.2478/geoca-2019-0030

Wang X., Griffin W.L., Chen J., Huang P. & Li X. 2011: U and Th contents and Th/U ratios of zircon in felsic and mafic magmatic rocks: improved zircon–melt distribution coefficient. *Acta Geol. Sinica (English Edition)* 85(1), 164–174. https://doi.org/ 10.1111/j.1733-6724.2011.00387.x

Watson E.B. & Harrison T.H. 1983: Zircon saturation revisited: temperature and composition effect in a variety of crustal magma types. *Earth Planet. Sci. Lett*. 64, 295–304.

Wiedenbeck M., Allé P., Corfu F., Griffin W.L., Meier M., Oberli F., von Quadt A., Roddick J.C. & Spiegel W. 1995: Three natural zircon standards for U-Th-Pb, Lu-Hf, trace element and REE analyses. *Geostandard Newslett.* 19, 1–23.

Williams I.S. 1998: U–Th–Pb geochronology by ion microprobe. In: McKissen M.A., Shanks III W.C. & Ridley W.S. (Eds.): Applications of microanalytical techniques to understanding mineralizing processes. *Rev. Econ. Geol.* 7, 1–35.

Winchester J.A. & Floyd P.A. 1977: Geochemical discrimination of different magma series and differentiation products using immobile elements. *Chem. Geol*. 20, 325—343.

Supplement

Table S1: Major (wt. %) and trace element concentrations (ppm) in the Permian volcanic rocks. *Abbreviations:* n.d. – not determined, -- below detection limit, * all Fe as Fe_2O_3.

sample		**T-1**	**T-13A**	**T-13B**
SiO_2	wt. %	54.58	52.64	52.52
Al_2O_3		16.63	15.74	16.19
TiO_2		0.59	1.613	1.703
Cr_2O_3		0.034	0.028	0.030
Fe_2O_3		*5.32	9.02	9.13
FeO		n.d.	3.41	3.02
MgO		3.88	6.27	6.52
MnO		0.08	0.121	0.117
CaO		3.54	6.96	4.73
Na_2O		4.78	3.09	4.00
K_2O		3.46	0.17	0.42
P_2O_5		0.23	0.31	0.32
Total		93.12	95.96	95.68
LOI		6.70	0.67	0.75
Ni	ppm	65	79	83
Sc		11	22	22
Ba		282	44	86
Co		18.2	n.d.	n.d.
Cs		12.5	n.d.	n.d.
Ga		15.2	n.d.	n.d.
Hf		4	4.5	4.5
Nb		9.9	14	13
Rb		119	12	21
Sn		3	n.d.	n.d.
Sr		115	686	319
Ta		2.1	2	2
Th		7.7	4	4
U		2.3	2.8	2.9
V		88	171	185
W		1.2	n.d.	n.d.
Zr		154	200	184
Y		19.9	28	29
La		26.5	29	31
Ce		60	55	52
Pr		7.9	5	5
Nd		32.5	31	33
Sm		5.97	6	6
Eu		1.32	1.6	1.7
Gd		4.87	6.8	7.1
Tb		0.67	0.8	0.9
Dy		3.41	5	5.6
Ho		0.65	1.4	1.4
Er		1.75	3.4	3.4
Tm		0.27	0.5	0.5
Yb		1.56	2.7	2.8
Lu		0.24	0.5	0.47
C_{tot}	%	1.41	n.d.	n.d.
S_{tot}	%	--	0.01	0.03
Eu/Eu*		0.748	0.766	0.796
Zr/Y		7.72	7.14	6.35
Th/Yb		4.94	1.48	1.43
La_N/Yb_N		12.18	7.70	7.94

Table S2: Microprobe analyses of detrital plagioclases from the sample *T-3*.

sample **analyse**	**T-3** **10**	**T-3** **11**	**T-3** **12**	**T-3** **13**	**T-3** **17**	**T-3** **19**
SiO_2	65.10	65.10	65.54	64.92	67.16	66.19
Al_2O_3	21.68	21.68	22.8	22.46	20.95	22.16
FeO	0.0	0.08	0.06	0.06	0.0	0.04
MgO	0.0	0.02	0.0	0.0	0.0	0.01
CaO	2.61	2.56	2.82	3.28	1.77	2.81
Na_2O	10.1	10.2	9.99	9.71	10.56	10.00
K_2O	0.29	0.31	0.28	0.23	0.08	0.33
BaO	0.03	0.004	0.02	0.03	0.0	0.0
SrO	0.09	0.04	0.06	0.02	0.07	0.01
Total	99.84	99.82	100.80	100.76	100.58	101.55
Si	2.872	2.870	2.844	2.843	2.927	2.870
Al	1.127	1.126	1.166	1.159	1.076	1.132
Fe	0.000	0.003	0.002	0.002	0.000	0.001
Mg	0.000	0.001	0.000	0.000	0.000	0.001
Ca	0.123	0.121	0.131	0.154	0.083	0.131
Na	0.864	0.872	0.840	0.824	0.892	0.841
K	0.016	0.017	0.015	0.013	0.004	0.018
Ba	0.001	0.000	0.000	0.001	0.000	0.000
Sr	0.002	0.001	0.002	0.001	0.002	0.000
CatSum	5.005	5.012	5.001	4.996	4.984	4.994
Or %	1.6	1.7	1.6	1.3	0.5	1.8
Ab %	86.1	86.3	85.1	83.2	91.1	85.0
An %	12.3	12.0	13.3	15.5	8.4	13.2

Table S3: Microprobe analyses of detrital muscovites from the sample *T-3*.

Samples analyse	**T-3 1**	**T-3 2**	**T-3 3**	**T-3 4**	**T-3 5**	**T-3 7**	**T-3 8**	**T-3 14**	**T-3 15**	**T-3 16**
SiO_2	47.42	47.40	47.35	52.00	50.62	53.66	51.68	50.51	52.38	47.99
TiO_2	0.26	0.39	0.75	0.27	0.38	0.05	0.26	0.21	0.12	0.65
Al_2O_3	36.00	36.04	35.81	23.52	25.67	22.06	26.12	33.18	25.30	35.64
Cr_2O_3	0.04	0.00	0.00	0.04	0.01	0.00	0.00	0.04	0.00	0.06
FeO	0.66	0.61	0.74	4.61	3.72	4.87	4.17	0.95	3.22	0.68
BaO	0.05	0.24	0.04	0.10	0.17	0.03	0.10	0.10	0.04	0.12
MnO	0.00	0.01	0.00	0.04	0.01	0.01	0.02	0.00	0.01	0.01
MgO	0.40	0.37	0.62	4.05	3.12	4.72	3.36	1.30	3.73	0.42
CaO	0.01	0.00	0.03	0.01	0.00	0.00	0.01	0.01	0.03	0.01
Na_2O	0.47	0.53	0.57	0.02	0.06	0.03	0.05	0.13	0.08	0.41
K_2O	10.57	10.62	10.48	11.46	11.38	11.24	11.02	9.84	10.94	10.36
F	0.00	0.02	0.00	0.03	0.00	0.00	0.06	0.06	0.00	0.00
Cl	0.00	0.00	0.00	0.00	0.00	0.00	0.00	0.01	0.01	0.00
Total	95.88	96.23	96.39	96.16	95.14	96.67	96.86	96.33	95.85	96.35
O=Cl	0.00	0.00	0.00	0.00	0.00	0.00	0.00	0.00	0.00	0.00
O=F	0.00	0.01	0.00	0.01	0.00	0.00	0.02	0.02	0.00	0.00
Σ corr.	95.88	96.22	96.39	96.15	95.14	96.67	96.83	96.30	95.84	96.35
Si	6.236	6.223	6.202	7.002	6.859	7.167	6.863	6.563	6.983	6.273
$^{(IV)}Al$	1.764	1.777	1.798	0.998	1.141	0.833	1.137	1.437	1.017	1.727
Sum T	8	8	8	8	8	8	8	8	8	8
$^{(VI)}Al$	3.82	3.80	3.73	2.73	2.96	2.64	2.95	3.64	2.96	3.76
Ti	0.026	0.038	0.074	0.027	0.039	0.005	0.026	0.020	0.012	0.064
Cr	0.004	0.000	0.000	0.004	0.001	0.000	0.000	0.004	0.000	0.006
Li	0.000	0.000	0.000	0.000	0.000	0.000	0.000	0.000	0.000	0.000
Fe^{2+}	0.073	0.067	0.081	0.519	0.421	0.544	0.463	0.103	0.359	0.074
Mn	0.000	0.002	0.000	0.004	0.001	0.001	0.002	0.000	0.002	0.001
Mg	0.078	0.072	0.121	0.814	0.629	0.939	0.666	0.252	0.741	0.082
Sum M	4	4	4	4	4	4	4	4	4	4
Ca	0.001	0.000	0.004	0.001	0.000	0.000	0.001	0.002	0.004	0.001
Ba	0.002	0.012	0.002	0.005	0.009	0.002	0.005	0.005	0.002	0.006
Sr	0.000	0.000	0.000	0.000	0.000	0.000	0.000	0.000	0.000	0.000
Na	0.119	0.135	0.145	0.006	0.017	0.009	0.013	0.032	0.020	0.105
K	1.774	1.778	1.752	1.969	1.968	1.914	1.868	1.630	1.860	1.728
Sum X	2	2	2	2	2	2	2	2	2	2

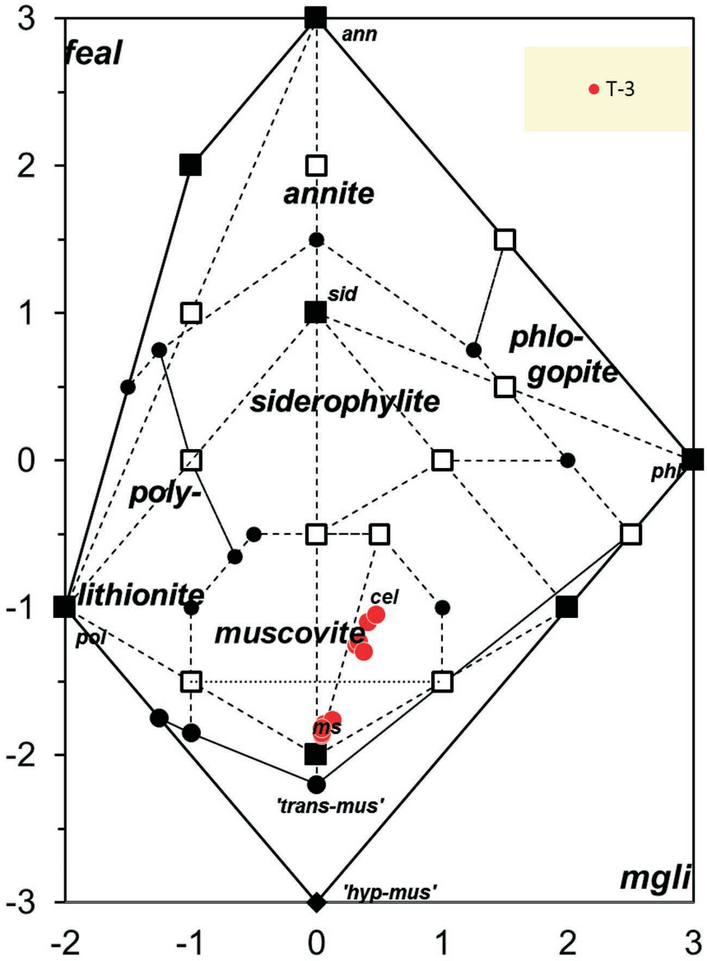

Fig. S1: *T-3* detrital micas in Tischendorf et al. (2007) classification diagram.